NIH Public Access
Author Manuscript
Neuron. Author manuscript; available in PMC 2010 August 13.

Published in final edited form as:
Neuron. 2009 August 13; 63(3): 316–328. doi:10.1016/j.neuron.2009.07.019.

Overexpression of IGF-1 in Muscle Attenuates Disease in a Mouse Model of Spinal and Bulbar Muscular Atrophy

Isabella Palazzolo[1,2], **Conor Stack**[1], **Lingling Kong**[3], **Antonio Musaro**[4], **Hiroaki Adachi**[5], **Masahisa Katsuno**[5,6], **Gen Sobue**[5], **J. Paul Taylor**[7], **Charlotte Sumner**[3], **Kenneth Fischbeck**[1], and **Maria Pennuto**[8,9,*]

[1]Neurogenetics Branch, NINDS, NIH, Bethesda, MD USA

[2]Istituto di Endocrinologia, Universita` degli Studi di Milano, Milan, Italy.

[3]Department of Neurology, Johns Hopkins School of Medicine, Baltimore, MD USA

[4]Institute Pasteur Cenci-Bolognetti, Department of Histology and Medical Embryology, IIM, Sapienza University of Rome, Italy

[5]Department of Neurology, Nagoya University Graduate School of Medicine, Nagoya, Japan

[6]Institute of Advanced Research, Nagoya University, Nagoya, Japan

[7]Department of Developmental Neurobiology, St. Jude Children's Research Hospital, Memphis, TN USA

[8]Department of Neurology, University of Pennsylvania School of Medicine, Philadelphia, PA USA

[9]Department of Neuroscience and Brain Technologies, Italian Institute of Technology, Genoa, Italy

SUMMARY

Expansion of a polyglutamine tract in the androgen receptor (AR) causes spinal and bulbar muscular atrophy (SBMA). We have previously shown that Akt-mediated phosphorylation of AR reduces ligand binding and attenuates the toxicity of mutant AR. Here we show that in cultured cells insulin-like growth factor 1 (IGF-1) reduces AR aggregation and increases AR clearance via the ubiquitin-proteasome system through phosphorylation of AR by Akt. To evaluate the potential benefit of exogenous IGF-1 *in vivo*, we crossed SBMA mice with mice that overexpress a muscle-specific isoform of IGF-1 selectively in skeletal muscle. In the resulting offspring, we found evidence of increased Akt activation and AR phosphorylation and decreased AR aggregation. Augmentation of IGF-1/Akt signaling rescued behavioral and histopathological abnormalities, extended the life span and reduced both muscle and spinal cord pathology of SBMA mice. This study establishes IGF-1/Akt-mediated inactivation of mutant AR as a strategy to counteract disease *in vivo* and demonstrates for the first time that skeletal muscle is a viable target tissue for therapeutic intervention in SBMA.

© 2009 Elsevier Inc. All rights reserved.

*Corresponding author: Maria Pennuto, Department of Neuroscience, Italian Institute of Technology, Genova, 16163, Italy, maria.pennuto@iit.it.

Publisher's Disclaimer: This is a PDF file of an unedited manuscript that has been accepted for publication. As a service to our customers we are providing this early version of the manuscript. The manuscript will undergo copyediting, typesetting, and review of the resulting proof before it is published in its final citable form. Please note that during the production process errors may be discovered which could affect the content, and all legal disclaimers that apply to the journal pertain.

NIH-PA Author Manuscript
NIH-PA Author Manuscript
NIH-PA Author Manuscript

NIH-PA Author Manuscript

NIH-PA Author Manuscript

NIH-PA Author Manuscript

Keywords

Polyglutamine disease; spinal and bulbar muscular atrophy; androgen receptor; insulin-like growth factor 1; skeletal muscle

INTRODUCTION

Spinal and bulbar muscular atrophy (SBMA), or Kennedy's disease, is an X-linked neurodegenerative disease caused by expansion of a CAG repeat encoding polyglutamine in the first exon of the androgen receptor (AR) gene (La Spada et al., 1991). The repeat is polymorphic in length, and individuals with an expansion over 36 residues develop disease. Expansion of polyglutamine is the cause of at least eight other neurodegenerative disorders, including Huntington's disease, dentatorubral and pallidoluysian atrophy, and six types of spinocerebellar ataxia (Orr and Zoghbi, 2007). A hallmark of the polyglutamine diseases is the accumulation of mutant protein into aggregates and inclusions, which can be detected using biochemical and histopathological techniques, respectively (Li et al., 2007; Ross and Poirier, 2004; Taylor et al., 2003). Although common features are shared by the polyglutamine diseases, different populations of neurons are vulnerable to each of the mutant proteins, resulting in clinically distinct disease manifestations.

Expansion of polyglutamine in AR causes loss of lower motor neurons in the brainstem and spinal cord, together with weakness, fasciculations and muscle atrophy (Katsuno et al., 2006). SBMA is a gender-specific disease, with only males fully affected. Females, even if homozygous for the mutation, have few if any symptoms (Schmidt et al., 2002). In both transgenic and knock in mouse models of SBMA, male but not female mice expressing mutant AR develop full disease manifestations (Katsuno et al., 2002; Yu et al., 2006). Importantly, reduction of testosterone levels in male mice ameliorates disease manifestations, suggesting a potential therapy for SBMA (Katsuno et al., 2003). Indeed, a phase 2 clinical trial shows benefits of androgen deprivation by leuprorelin acetate (Banno et al., 2009). However, the use of anti-androgens as therapy may have undesired side-effects.

Emerging evidence suggests a role for muscle in SBMA pathogenesis. Histological and molecular signs of muscle pathology are detectable before the appearance of pathological abnormalities in the spinal cord in a knock in mouse model of SBMA (Yu et al., 2006), suggesting that mutant AR may exert a direct toxic effect on skeletal muscle. In support of this notion is the observation that overexpression of normal AR in the skeletal muscle induces a phenotype similar to SBMA (Monks et al., 2007). Analysis of muscle biopsy samples derived from SBMA patients suggests a mixed pathology with both myopathic and neurogenic features (Soraru et al., 2008). Although the extent to which weakness in SBMA is a consequence of motor neuron degeneration with denervation and secondary muscle atrophy, or primary muscle degeneration with secondary effects on the motor neurons is unknown, these observations suggest that skeletal muscle may be an important target for disease treatment (Jordan and Lieberman, 2008). Among the protective factors that help maintain muscle integrity, insulin-like growth factor 1 (IGF-1) has been shown to have an anabolic effect on skeletal muscle (reviewed by Sandri, 2008). Transgenic mice that overexpress a muscle isoform of IGF-1 (mIGF-1) selectively in skeletal muscle develop extensive muscle hypertrophy (Musaro et al., 2001). IGF-1 induces muscle regeneration by stimulating the proliferation of satellite cells in normal (Musaro et al., 2001) and pathological conditions, such as amyotrophic lateral sclerosis (Dobrowolny et al., 2005). At the molecular level, IGF-1 promotes muscle hypertrophy through activation of the phosphatidyl-inositol 3-kinase (PI3K)/Akt pathway (Rommel et al., 2001). Beyond the general potential benefit for IGF-1 in myopathic conditions, there is a specific rationale for IGF-1 in the treatment of SBMA based on its ability to inactivate the AR through

NIH-PA Author Manuscript

NIH-PA Author Manuscript

NIH-PA Author Manuscript

an Akt-dependent mechanism (Palazzolo et al., 2007). We have previously shown that phosphorylation of AR by Akt blocks ligand binding, thus reducing ligand-induced nuclear translocation and transactivation of AR in cell culture. Moreover, we have shown that IGF-1 reduces mutant AR toxicity in cultured cells through phosphorylation of AR at the Akt consensus sites. These observations suggest IGF-1 and Akt-mediated inactivation of AR as potential therapy for SBMA.

Here, we report that augmentation of IGF-1 levels decreases mutant AR aggregation and increases AR clearance through the ubiquitin-proteasome system, and that this effect is dependent on AR phosphorylation by Akt. In a mouse model of SBMA, muscle-specific overexpression of IGF-1 activates Akt and increases AR phosphorylation at Akt consensus sites. This correlates with decreased AR aggregation in both the muscle and spinal cord. Furthermore, overexpression of IGF-1 rescues behavioral and histopathological abnormalities, delays disease onset, and prolongs the life span of SBMA mice. Importantly, IGF-1 attenuates both the morphological and molecular signs of myopathic and neurogenic muscle pathology and increases motor neuron survival. Our results highlight a disease-specific mechanism of action of IGF-1 in SBMA muscle, which likely involves phosphorylation and inactivation of AR by Akt and presents an opportunity to mitigate the disease manifestations *in vivo*. Moreover, our study indicates that muscle is a reasonable target tissue and highlights IGF-1 as a promising therapy for SBMA.

RESULTS

IGF-1 Reduces Mutant AR Aggregation in Cell Culture through Phosphorylation by Akt

Binding of ligand induces aggregation of mutant AR (Katsuno et al., 2002; Stenoien et al., 1999). Here, we define AR aggregates as the high molecular weight oligomers soluble in RIPA buffer after high-speed centrifugation and sonication. These species are detected as a smear in the stacking portion of SDS-polyacrylamide gels and are retained in the acetate membrane in filter retardation assay, as previously described (Li et al., 2007; Rusmini et al., 2007; Taylor et al., 2003; Williams et al., 2009). We previously showed that phosphorylation of AR by Akt impairs ligand binding (Palazzolo et al., 2007). Therefore, we hypothesized that agents which activate Akt such as IGF-1 would attenuate ligand-dependent AR aggregation. To test this, we used COS1 cells transiently transfected with a vector expressing a mutant AR with 65 glutamine residues (AR65Q) (Figure 1A). The cells were treated with the AR ligand dihydrotestosterone (DHT) with or without IGF-1 supplementation. Treatment of the cells with DHT increased the accumulation of high molecular weight AR species 2.3 fold (Figure 1A, left panel). Treatment of the cells with IGF-1 increased phosphorylation of Akt at serine 473, which is critical for Akt activation (Figure 1A, right panel) (Alessi et al., 1996), and reduced basal and ligand-induced AR aggregation by 100% and 80%, respectively (Figure 1A, left panel). Consistent with this finding, treatment of the cells with IGF-1 decreased the amount of AR retained in filter retardation assay by 68% (Figure 1A, bottom panel). The effect of IGF-1 on AR aggregation was not due to decreased transcription of AR since transcript levels were unchanged (data not shown). Similar results were obtained in transiently transfected C2C12 myoblast cells and stably transfected motor neuron-derived MN-1 cells (Supplemental Figure S1), indicating that the effect of IGF-1 on AR aggregation is independent of cell type.

Based on our previous findings (Palazzolo et al., 2007), we hypothesized that the ability of IGF-1 to suppress ligand-dependent AR aggregation was dependent on activation of the PI3K/Akt pathway and phosphorylation of AR by Akt. To test the role of PI3K, we used the specific PI3K inhibitor LY294002 (Figure 1A) (Vlahos et al., 1994). Treatment of the COS1 cells with LY294002 decreased the IGF-1-induced phosphorylation of Akt at serine 473 (Figure 1A, right panel) and blocked the effect of IGF-1 on AR aggregation as assayed by both western blotting and filter retardation assay (Figure 1A, left panel). AR has two serines that are consensus sites

NIH-PA Author Manuscript

NIH-PA Author Manuscript

NIH-PA Author Manuscript

for Akt, serine 215 and serine 792 (Lin et al., 2001). We have previously shown that Akt phosphorylates mutant AR at serine 215 (Palazzolo et al., 2007). To determine whether phosphorylation of AR by Akt reduces aggregation, we used AR variants in which serines 215 and 792 were substituted with either alanine, which cannot be phosphorylated, or aspartate, which mimics constitutive phosphorylation (Palazzolo et al., 2007). In COS1 cells, DHT increased the aggregation of both the unaltered AR65Q and the alanine-substituted (S215A,S792A) AR65Q by 1.5 and 1.9 fold, respectively, in western blotting (Figure 1B, upper panel), and by 5.8 and 4.9 fold, respectively, in filter retardation assay (Figure 1B, bottom panel). In contrast, DHT did not change the aggregation of the phospho-mimetic variant (S215D,S792D), suggesting that AR phosphorylation at Akt consensus sites prevents aggregation. To determine whether the effect of IGF-1 requires phosphorylation of AR at these serines, we transfected HEK293T cells with either unaltered AR65Q or the alanine-substituted receptor, and treated the cells with DHT and IGF-1 (Figure 1C). IGF-1 decreased AR-positive aggregates by 43% in cells expressing AR65Q, but did not have any effect in cells expressing the alanine-substituted receptor. Together, these results show that IGF-1 reduces AR aggregation through activation of PI3K/Akt and at least in part through phosphorylation of AR by Akt.

IGF-1 Induces Mutant AR Clearance through the Ubiquitin-Proteasome System

Because the effect of IGF-1 on AR aggregation correlated with a decrease in the levels of the protein (Figure 1, white bars), we hypothesized that IGF-1/Akt signaling affects the stability of mutant AR. To test this, we expressed mutant AR in MN-1 cells and analyzed protein clearance in the presence of the protein synthesis inhibitor cycloheximide (CHX) (Figure 2A). Treatment of the cells with IGF-1 significantly increased the clearance of AR as compared to the vehicle-treated samples. To determine whether phosphorylation by Akt influences AR clearance, we analyzed the stability of the phospho-defective AR-S215A,S792A variant (Figure 2B). Loss of AR phosphorylation significantly reduced the rate of AR clearance, suggesting that phosphorylation of AR at the Akt consensus sites is important for AR degradation.

Next, we sought to determine which pathway is responsible for the IGF-1 effect on AR clearance. We have previously shown that phosphorylation by Akt induces AR degradation through the proteasome (Palazzolo et al., 2007). Consistent with this, treatment of the cells with the proteasome inhibitor MG132 blocked the effect of IGF-1 in a dose-dependent fashion (Figure 2C). Proteins degraded through the proteasome are ubiquitylated. Therefore, we asked whether mutant AR ubiquitylation is influenced by phosphorylation. To address this, we expressed either non-substituted or phospho-defective AR in HEK293T cells together with vector expressing HA-ubiquitin and processed the cells for immunoprecipitation with anti-AR antibody (Figure 2D). The ubiquitylation of the phospho-defective AR was lower than that of the non-substituted receptor. To determine whether IGF-1 induces AR clearance through other pathways, we surveyed the target of rapamycin TOR, which is activated by IGF-1 and induces autophagy (Sarbassov et al., 2005). Treatment of the cells with rapamycin reduced the phosphorylation of the downstream effector of TOR, S6K p70, but had no effect on AR clearance (Supplemental Figure S2). Together, these results indicate that IGF-1 increases mutant AR clearance through the ubiquitin-proteasome system in a phosphorylation-dependent manner.

IGF-1 Activates Akt and Increases AR Phosphorylation at Serine 215 in SBMA Muscle

To test the effect of IGF-1 *in vivo*, we crossed mice that express human full length AR with 97 glutamine residues (AR97Q) and that recapitulate the myogenic changes and the neurogenic signs of muscle pathology observed in SBMA patients (Katsuno et al., 2002) (Figure 7) with mice that overexpress a rat non-circulating, muscle-specific isoform of IGF-1 (mIGF-1) under

NIH-PA Author Manuscript

NIH-PA Author Manuscript

NIH-PA Author Manuscript

the control of the rat myosin light chain promoter (Musaro et al., 2001). The mIGF-1 mice show increased muscle mass and strength, reduced age-related muscle loss, and augmented regenerative capacity of muscle. To characterize the AR97Q/mIGF-1 double transgenic mice, we analyzed the expression of the mIGF-1 and AR transgenes. The mRNA levels of the rat mIGF-1 and human AR transgenes were measured by real-time PCR and normalized to phosphoglycerate kinase 1 (PGK1) mRNA (Figure 3A) and 18S rRNA (data not shown). In the skeletal muscle, mIGF-1 mRNA was detected in both mIGF-1 and AR97Q/mIGF-1 mice, but not wild type and AR97Q mice (Figure 3A, left panel). No expression of mIGF-1 was detected in the spinal cord (Supplemental Figure S3A, left panel). The human AR transgene is expressed at similar levels in AR97Q and AR97Q/mIGF-1 mice both in muscle (Figure 3A, right panel) and spinal cord (Supplemental Figure S3A, right panel), indicating that mIGF-1 does not alter AR expression in this mouse model.

To determine whether the mIGF-1 is biologically active, we analyzed the phosphorylation of Akt at serine 473 and of AR at serine 215 in muscle and spinal cord. Overexpression of mIGF-1 resulted in augmented phosphorylation of Akt (Figure 3B, left panel) and endogenous mouse AR (Figure 3B, right panel) in the muscle, but not spinal cord (Supplemental Figure S3B) of both mIGF-1 and AR97Q/mIGF-1 mice. Under these experimental conditions, we could not clearly detect phosphorylation of transgenic human expanded polyglutamine AR. One explanation for this is that when phosphorylated by Akt, mutant AR is targeted for degradation through the proteasome (Figure 2) (Palazzolo et al., 2007). Thus, we injected the skeletal muscle of AR97Q and AR97Q/mIGF-1 mice with the proteasome inhibitor velcade for 24 hours to block mutant AR degradation (Bonuccelli et al., 2007), and analyzed AR phosphorylation by western blotting (Figure 3C). In the velcade-treated muscle, phosphorylation of mutant AR was increased by 4.3 fold in AR97Q/mIGF-1 mice as compared to AR97Q mice. Together, these data indicate that overexpression of mIGF-1 in AR97Q mice results in Akt activation and phosphorylation of AR at the Akt consensus site serine 215.

Overexpression of mIGF-1 Reduces Mutant AR Aggregation in SBMA Muscle

Because we have found that IGF-1/Akt signaling reduces polyglutamine AR aggregation in cultured cells (Figure 1), we asked whether mIGF-1 decreases the accumulation of AR-positive aggregates *in vivo*. To test this, we analyzed protein lysates from skeletal muscle of AR97Q and AR97Q/mIGF-1 mice by western blotting (Figure 4A) and filter retardation assay (Figure 4B). In AR97Q mice, high molecular weight AR species were not detected at 6 weeks of age (Supplemental Figure S4A), but they were detected starting at 12 weeks of age (Figure 4), indicating that appearance of these species correlates with disease progression (Figure 5 and Figure 6). By contrary, in AR97Q/mIGF-1 mice these species were not detected before 24 weeks of age (Supplemental Figure S4A). To further characterize the high molecular weight AR species, we electrophoresed the muscle lysates on a 1.5% SDS-agarose gel, which resolves large protein complexes (Figure 4C) (Bagriantsev et al., 2006;Williams et al., 2009). High molecular weight AR species were detected in 12 weeks old AR97Q mice, and to a lesser extent in AR97Q/mIGF-1 mice. To determine the size of these species, we analyzed the muscle lysates by size-exclusion chromatography followed by SDS-polyacrylamide gel electrophoresis (Figure 4D). Although the molecular weight of monomeric mutant AR is about 130 kDa and eluted in fraction 9 (Figure 4D, asterisk), in AR97Q mice AR eluted mostly as high molecular weight species with a peak in between 440 and 2000 kDa. Importantly, IGF-1 reduced by 3 fold the amount of AR eluting off as high molecular weight species.

To determine whether mIGF-1 decreases nuclear accumulation of diffused AR and nuclear inclusions, longitudinal and cross sections of quadriceps muscle of AR97Q and AR97Q/mIGF-1 mice were stained with 1C2 antibody (Figure 4E). Diffuse nuclear staining and AR-positive nuclear inclusions were evident in AR97Q mice. Overexpression of mIGF-1 in AR97Q

NIH-PA Author Manuscript

NIH-PA Author Manuscript

NIH-PA Author Manuscript

muscle resulted in significantly less accumulation of mutant AR in nuclear inclusions. The effect of mIGF-1 on AR aggregation and nuclear accumulation suggests a protective role of the PI3K/Akt pathway in SBMA.

mIGF-1 Delays Disease Onset and Extends Disease Duration and Survival of SBMA Mice

We monitored the effect of overexpression of mIGF-1 on disease onset (Figure 5A), disease duration (Figure 5B), and survival (Figure 5C) of SBMA mice. Disease onset was defined as the week in which the mouse loses 5% body weight for at least two consecutive weeks, while disease duration was calculated as the number of weeks from disease onset to death. mIGF-1 delayed the median disease onset by 10.5 weeks (χ^2LR = 11.4, p = 0.0007) and extended the median disease duration by 20 weeks (χ^2LR = 10.7, p = 0.001). To assess the effect of mIGF-1 on survival, we monitored the life span of AR97Q and AR97Q/mIGF-1 mice for 64 weeks. Analysis of the survival curves indicated that mIGF-1 extended the median life span by 30 weeks (χ^2LR = 10.2, p = 0.001). These data show that mIGF-1 delays disease onset and extends disease duration and life span in SBMA mice. Similar results were obtained without censoring of the data (Supplemental Figure S5).

Overexpression of mIGF-1 Attenuates Disease Manifestations in SBMA Mice

To characterize in detail the effect of overexpression of mIGF-1 on SBMA pathogenesis, we analyzed body weight and motor function. AR97Q/mIGF-1 mice did not show the severe muscle wasting and reduced body size observed in AR97Q littermates (Figure 6A). Notably, AR97Q/mIGF-1 mice lost body weight significantly later than AR97Q mice (p = 0.001; n = 15) (Figure 6B). In addition, we assessed muscle strength by hanging wire test (Figure 6C) and motor performance by rotarod (Figure 6D) and footprinting (Figure 6E) tasks. By hanging wire test, AR97Q mice showed progressive deterioration in performance starting from 12 weeks of age when compared to wild type mice (p = 0.001, n = 15). In contrast, AR97Q/mIGF-1 performed significantly better (p = 0.001; n = 15). By rotarod task, AR97Q mice showed significant performance deficits compared to wild type mice starting at 16 weeks of age (p = 0.01, n = 7). These deficits were rescued by overexpression of mIGF-1. On footprint analysis, AR97Q mice dragged their hind legs, whereas AR97Q/mIGF-1 mice did not show gait abnormality. Moreover, AR97Q/mIGF-1 mice showed increased activity, interest in exploration of the surrounding space, and ability to turn their bodies when suspended by the tail compared to age-matched AR97Q mice (data not shown). Altogether, these results show that mIGF-1 reduces muscle weakness and improves motor function in SBMA mice.

mIGF-1 Ameliorates SBMA Muscle Pathology

To address whether overexpression of mIGF-1 has an effect on muscle denervation and myopathy in SBMA mice, we performed histological analysis of transverse sections of quadriceps muscles using hematoxylin and eosin (Figure 7A) and nicotinamide adenine dinucleotide (Figure 7B) staining. At 12 weeks of age, AR97Q mice showed signs of muscle denervation, such as grouped and angulated atrophic fibers (Figure 7A, asterisk), target fibers (Figure 7B, arrow) and moth-eaten fibers (Figure 7B, asterisk), and of muscle myopathy, such as the presence of large fibers with central nuclei (Figure 7A, arrow), which indicate muscle degeneration and regeneration (Musaro et al., 2001). In contrast, mIGF-1 expression counteracted muscle atrophy and degeneration and preserved myofibers architecture (Figure 7A and B). This amelioration of muscle pathology was sustained even at 24 weeks of age (Supplemental Figure S6).

To further characterize the effect of mIGF-1 on SBMA muscle, we analyzed by real-time PCR the expression of genes upregulated during denervation, such as runx 1 (AML1), myogenin, embryonal and perinatal myosin heavy chain, and the alpha subunit of the acetylcholine receptor (Figure 7C) (Kostrominova et al., 2005; Zhu et al., 1994). Consistent with the

NIH-PA Author Manuscript

NIH-PA Author Manuscript

NIH-PA Author Manuscript

pathological findings, these genes were all upregulated in AR97Q mice at 12 weeks of age (Figure 7C, white bars), and induction correlated with disease progression (Supplemental Figure S7). Importantly, expression of these genes was also increased in skeletal muscle autopsy specimens of four SBMA patients compared to unaffected controls (Figure 7C, black bars). Overexpression of mIGF-1 in the muscle of SBMA mice significantly attenuated the induction of these markers. Altogether, these results indicate that mIGF-1 prevents muscle denervation and degeneration in SBMA mice.

Overexpression of mIGF-1 in SBMA Muscle Reduces Motor Neuron Loss

IGF-1 has a trophic effect on motor neurons (reviewed by Cary and La Spada, 2008), and increased IGF-1/Akt signaling in the muscle has previously been shown to improve motor neuron survival in amyotrophic lateral sclerosis (Dobrowolny et al., 2005; Kaspar et al., 2003). Therefore, we hypothesized that overexpression of mIGF-1 in muscle protects motor neurons from damage caused by mutant AR. To test this, we analyzed ventral spinal cord pathology by Nissl staining (Figure 8A). Histological analysis revealed that in AR97Q mice the number of motor neurons/section was reduced by 27 ± 9% compared to wild type mice (8.4 ± 0.3 and 11.6 ± 1 motor neurons/section, respectively), although this difference was not statistically significant ($p = 0.07$, $n = 3$ animals). mIGF-1 restored the number of motor neurons to levels comparable to wild type mice (11.5 ± 2). This result was validated by the analysis of the motor neuron marker choline acetyltransferase (ChAT). We found that ChAT levels were increased in AR97Q/mIGF-1 mice by 1.5 ± 0.2 fold compared to AR97Q mice, further suggesting that mIGF-1 promotes survival of motor neurons in SBMA mice (Figure 8B).

Another sign of motor neuron degeneration in SBMA mice is the reduction of the cross-sectional area of motor neurons (Katsuno et al., 2002). Therefore, we measured the area of anterior horn motor neurons in Nissl-stained spinal cord sections (Figure 8C). The median area of motor neurons in AR97Q mice (253.5 μm^2) was significantly ($W = 6097$, $p = 0.01$, n motor neurons = 100) smaller than that of wild type mice (277 μm^2), but rescued in AR97Q/mIGF-1 mice (290 μm^2, $W = 4676.5$, $p = 0.43$).

Polyglutamine AR forms aggregates in the spinal cord (Katsuno et al., 2002). We asked whether the beneficial effect of mIGF-1 on motor neurons correlated with a decrease in AR aggregation. Western analysis of spinal cord lysates showed that overexpression of mIGF-1 in the muscle reduced AR aggregation in 12 and 24 weeks old mice (Figure 8D and Supplemental Figure S4B). AR-positive aggregates were detected in AR97Q/mIGF-1 mice starting from 40 weeks of age. These results indicate that AR aggregates appear in the spinal cord of AR97Q/mIGF-1 mice at later stages of disease as compared to muscle.

To determine whether overexpression of mIGF-1 reduces mutant AR-positive inclusions in the nuclei of motor neurons, we analyzed 1C2-positive staining in cross sections of ventral spinal cord of AR97Q and AR97Q/mIGF-1 mice (Figure 8E). Nuclear 1C2-positive inclusions were decreased in AR97Q/mIGF-1 mice compared to AR97Q mice. Altogether, these results indicate that overexpression of mIGF-1 in the skeletal muscle attenuates spinal cord pathology in SBMA mice.

In conclusion, the data presented here show that IGF-1/Akt signaling promotes AR phosphorylation, reduces AR aggregation by stimulating protein clearance, and ameliorates disease manifestations in SBMA mice. Moreover, our results indicate that IGF-1-mediated inactivation of mutant AR is a potential therapy for SBMA and suggest muscle as a target tissue for intervention.

NIH-PA Author Manuscript

NIH-PA Author Manuscript

NIH-PA Author Manuscript

DISCUSSION

We describe the effect of mIGF-1 on SBMA pathogenesis. We previously showed that IGF-1 protects cultured cells from the toxicity of expanded polyglutamine AR through activation of Akt and induction of AR phosphorylation (Palazzolo et al., 2007). In this study, we extended these findings by showing that phosphorylation of AR by IGF-1/Akt signaling increases protein clearance through the proteasome and reduces mutant AR aggregation in cultured cells. Muscle-specific overexpression of mIGF-1 in SBMA mice induced phosphorylation of AR at the Akt consensus site serine 215 and reduced mutant AR aggregation in the muscle. mIGF-1 significantly improved motor performance and body weight, counteracted muscle and spinal cord pathology, and extended survival. We propose that mIGF-1 inactivates mutant AR through phosphorylation by Akt, and that this results in reduced muscle denervation and degeneration. Our results represent the first evidence that muscle is a therapeutic target in SBMA and provide the rationale for the use of mIGF-1 as a novel therapy for SBMA.

Phosphorylation of AR by mIGF-1/Akt Signaling and Toxicity

Overexpression of mIGF-1 attenuates disease manifestations in SBMA mice. One possible mechanism involves a direct effect of mIGF-1 on polyglutamine AR. AR has two serines, serine 215 and serine 792, that conform to the Akt consensus site (Lawlor and Alessi, 2001) and are conserved through evolution (Palazzolo et al., 2007). We have previously shown that phosphorylation of mutant AR by Akt decreases ligand binding, thus inhibiting ligand-dependent protein stabilization, nuclear translocation, transcription activation, and most importantly toxicity in cultured cells (Palazzolo et al., 2007). Akt phosphorylates other polyglutamine disease proteins. For example, phosphorylation of mutant huntingtin at serine 421 is protective in cultured striatal neurons (Humbert et al., 2002). Here, we show that phosphorylation of mutant AR by Akt results in decreased aggregation both *in vitro* and *in vivo*, and this correlates with reduced toxicity in a mouse model of SBMA. Importantly, we show that the mechanism by which IGF-1 reduces AR aggregation involves degradation of mutant AR through the proteasome in a process that is dependent on AR phosphorylation by Akt. These results are consistent with previous observations from Chang's group, which show that phosphorylation of non-expanded AR by Akt induces the degradation of the receptor through the proteasome (Lin et al., 2002). Our results suggest a specific effect of IGF-1 on AR, which involves inactivation of mutant AR through phosphorylation by Akt and decreased toxicity.

IGF-1 Promotes Muscle Hypertrophy and Inhibits Muscle Atrophy

IGF-1 can have additional effects that are independent of AR modifications. IGF-1 has long been established as an anabolic factor for the skeletal muscle (Florini et al., 1996). Overexpression of IGF-1 in muscle induces muscle hypertrophy and actively counteracts muscle atrophy (Coleman et al., 1995; Musaro et al., 2001; Sandri et al., 2004), with a mechanism that involves activation of PI3K/Akt signaling (Bodine et al., 2001; Rommel et al., 2001). Several downstream effectors of Akt have been shown to play a role in muscle atrophy. For instance, Akt inhibits FOXO, which in muscle promotes protein degradation via the ubiquitin-proteasome system (Sandri et al., 2004) and autophagy (Zhao et al., 2007). FOXO activates transcription of the ubiquitin ligases, atrogin1/MAFbx and MuRF1, and this process is inhibited by IGF-1 (Stitt et al., 2004). Because we did not find any change in expression of these genes in the mouse model of SBMA used in this study, this pathway is not likely to be relevant to SBMA (Palazzolo and Pennuto, unpublished results). Instead, it is possible that IGF-1 restores SBMA muscle via inhibition of FOXO and FOXO-induced autophagy. IGF-1/Akt signaling promotes muscle hypertrophy by inducing novel protein synthesis through inhibition of the glycogen synthase kinase 3β and activation of the mammalian target of

NIH-PA Author Manuscript

NIH-PA Author Manuscript

NIH-PA Author Manuscript

rapamycin (mTOR) (Bodine et al., 2001; Rommel et al., 2001). The contribution of these pathways to SBMA pathogenesis remains to be elucidated.

IGF-1 is a Trophic Factor for Motor Neurons

The rescue of morphological abnormalities that we observe in the spinal cord of SBMA mice suggests a trophic effect for mIGF-1 on motor neurons. IGF-1 promotes sprouting, axonal growth, and survival of embryonic motor neurons (Caroni and Grandes, 1990), and after nerve injury (Hughes et al., 1993; Neff et al., 1993). We have previously shown that IGF-1 is a pro-survival factor for motor neuron-derived cells that express expanded polyglutamine AR (Palazzolo et al., 2007). Therefore, it is possible that overexpression of mIGF-1 in the muscle of SBMA mice has direct beneficial effect on motor neurons. Also, muscle is itself a source of neurotrophic and growth factors that may have protective effect on motor neurons (reviewed by Cary and La Spada, 2008). Muscle-released brain-derived neurotrophic factor is retrogradely transported by motor neurons (DiStefano et al., 1992). Muscle-specific overexpression of mIGF-1 may stimulate the secretion of growth factors and neurotrophins from muscle, which in turn have beneficial effect on motor neurons. The decreased AR aggregation that we found in the spinal cord of AR97Q/mIGF-1 mice suggests a direct effect of mIGF-1 on AR. However, we did not observe a change in AR phosphorylation in the spinal cord of AR97Q/mIGF-1 mice compared to AR97Q mice.

The results that we describe in this study suggest mIGF-I as a good candidate for therapy in SBMA. Akt activation is predicted to result in a loss of AR function (Palazzolo et al., 2007), which in turn may alter fertility. However, we have found that overexpression of mIGF-1 selectively in muscle does not affect fertility of SBMA mice (Supplemental Figure S8). Subcutaneous injection of human recombinant IGF-1 has not been effective in ALS clinical trials (Borasio et al., 1998; Lai et al., 1997; Sorenson et al., 2008). However, the muscle-specific IGF-1 isoform used in this study may be more beneficial. Moreover, we provide evidence that, in contrast to ALS, IGF-1/Akt signaling has a direct inhibitory effect on the mutant protein, which helps to prevent motor neuron degeneration in SBMA.

EXPERIMENTAL PROCEDURES

Animals

All experiments were carried out in accordance with the National Institutes of Health Guide for the Care and Use of Laboratory Animals, and were approved by the NINDS Animal Care Committee. Mice were observed daily and sacrificed when they showed signs of muribundity (see below). AR97Q and AR97Q/mIGF-1 mice, as well as mIGF-1 and wild type mice used in the experiments described here were derived by crossing C57Bl6 mIGF-1 mice with BDF1 AR97Q mice. All the experiments were performed in male mice coming from the F1 generation of the cross described above. Similar to AR97Q, we crossed mice that express normal AR (AR24Q) (Katsuno et al., 2002) with mIGF-1 mice. Overexpression of IGF-1 in the skeletal muscle of AR24Q mice did not result in any change of behavior and survival (data not shown). Mice were genotyped by PCR on tail DNA as previously described (Katsuno et al., 2002; Musaro et al., 2001), using REDExtract-N-Amp Tissue PCR kit (Sigma) according to manufacturer’s instructions.

Behavioral and Survival Analysis

All the tests were performed weekly. Data were analyzed retrospectively. Rotarod analysis: Three trials were performed weekly using the Ugo Basile ROTA-ROD for mice (Ugo Basile). Mice were put on the rod at speed of 16 rpm for a maximum period of 180 seconds, and the best performance for each mouse was recorded. Hanging wire test: The mouse was placed on top of a wire cage lid. The lid was shaken slightly 3 times to cause the mouse to grip the wires

NIH-PA Author Manuscript

NIH-PA Author Manuscript

NIH-PA Author Manuscript

and then the lid was turned upside down. The latency to fall was recorded for a maximum time of 60 seconds (Crawley, 2008). Foot printing analysis: The forepaws and the hindpaws of the mouse were painted with red and blue colors, respectively, and the mouse was allowed to walk along a narrow, paper-covered corridor. Survival analysis: Moribundity was set as the time in which the mouse lost more than 30% and up to 35% of body weight, or showed inability to move, dehydration, and cachexia.

Human Skeletal Muscle Samples

This study was conducted according to the Declaration of Helsinki (Hong Kong Amendment). Autopsy sample collection was approved by the ethics committee of Nagoya University Graduate School of Medicine. Written informed consent was obtained from the family of each patient. Confidentiality was ensured by assigning a study code to each patient. All studies conformed to the ethics guidelines for human genome/gene analysis research and the ethics guidelines for epidemiological studies endorsed by the Japanese government. Anonymized control biopsy samples were obtained from Dr A. Lieberman (Ann Arbor, MI, US) following the University of Michigan IRB guidelines. A supplemental control Human Skeletal muscle total RNA has been purchased from Ambion/Applied Biosystems.

Taqman Quantitative PCR Analysis

Animals were anesthetized with isoflurane and sacrificed. Quadriceps muscles and spinal cord were flash frozen in liquid nitrogen. Total RNA was extracted with Trizol (Invitrogen) as previously described (Pennuto et al., 2008). One μg RNA was retro-transcribed using the cDNA Archive kit (Applied Biosystems) following manufacturer's instructions. Gene expression was measured by quantitative real-time PCR using ABI 9900 Sequence Detector System (Applied Biosystems). Specific assays on demand for myogenin (Mm_00446194-m1 and Hs_00231167-m1), embryonic (Mm_01332452-m1 and Hs_00159463-m1), perinatal (Mm_01329512-m1 and Hs_00267293-m1), and adult (Mm_01332489-m1 and Hs_00428600-m1) myosin heavy chain, acetylcholine receptor alpha (Mm_00431629-m1 and Hs_00175578-m1), runx1 (Mm_00486762-m1 and Hs_00231079-m1), human AR (Hs_00907244-m1), PGK1 (Mm_00435617-m1), and beta-glucuronidase (Hs_99999908-m1) were from Applied Biosystems. Rat mIGF1 transgene expression was measured using the following primers 5'-GCACTCTGCTTGCTCACCTTTA and 5'-CCCCGCAAAGGGTCTCT (Assay on Design, Applied Biosystems). The level of each transcript was measured with the threshold cycle (Ct) method using as endogenous controls PGK1 mRNA for mouse tissues and beta-glucuronidase mRNA for human tissues. Values were normalized to the mean of the wild type animals in each group, which was assigned as 1, unless differently indicated.

Biochemical Analysis

HEK293T, Cos1, and MN-1 cells were cultured and transfected as previously described (Palazzolo et al., 2007). Cells were treated with DHT (10 nM, 24 hours, Sigma), IGF-1 (100 ng/ml, 24–48 hours, Calbiochem), MG132 (1–10 μM, 16 hours, Calbiochem), cycloheximide (25 μM, Calbiochem), and LY294002 (10 μM, 24 hours, Calbiochem), as indicated. Cells were processed for western blotting as previously described (Palazzolo et al., 2007). Tissues were snap frozen in liquid nitrogen. Frozen tissue samples (50–100mg) were pulverized and homogenized in 500 μl RIPA buffer (150 mM NaCl, 6 mM Na_2HPO_4 , 4 mM NaH_2PO_4, 2 mM EDTA pH 8, 1% Sodium Deoxycholate, 0.5% TritonX100, 0.1% sodium dodecyl sulfate (SDS)) and protease inhibitor cocktail (Roche), sonicated for 10 seconds, and centrifuged 10 minutes at 15700 g at 4C. The soluble fraction was collected and total protein concentrations were determined by the bicinchoninic acid Protein Assay Kit (Pierce) following manufacturer's instructions. For western blotting, protein lysates (100 μg) were separated on 7.5% SDS-

NIH-PA Author Manuscript

NIH-PA Author Manuscript

NIH-PA Author Manuscript

polyacrylamide gels and transferred to PVDF membranes (Millipore). For the filter retardation assay, protein lysates (20 μg) were loaded onto acetate and nitrocellulose membranes and washed twice with phosphate buffered saline. For SDS-agarose gels, protein lysates (100 μg) were diluted in Laemmli buffer and loaded on 1.5% high melting agarose gels containing 1% SDS, as previously described (Bagriantsev et al., 2006). For size-exclusion chromatography, muscle lysates (3 mg/500 μl) were resolved on a Superdex 200 10/300 GL column (GE Healthcare BioSciences) at a flow rate of 0.3 ml/min in 0.5M phosphate buffer pH 7.4 using a Pharmacia P-500 series FPLC system. Fractions (0.6 ml) were concentrated with Amicon-Ultra4 50K filters (Millipore). To calibrate the column, high molecular weight standards (GE Healthcare BioSciences) were eluted under the same conditions. The void volume of the column was determined by eluting dextran blue (2000 kDa). To analyze phosphorylation, muscle lysates were prepared in lysis buffer (50 mM HEPES, 250 mM NaCl, 5 mM EDTA, 0.1% NP40) with protease and phosphatase inhibitor cocktails (Pierce). Membranes were probed with the following antibodies: anti-AR (N20) (sc-816, Santa Cruz), anti α-Tubulin (T6199, Sigma), anti-phospho-serine 473 Akt and total Akt (9271 and 9272, Cell Signaling), anti-polyglutamine 1C2 (MAB1574, Chemicon), anti-phospho-serine 215 AR (PA137082, Pierce), anti-actin (sc-1616, Santa Cruz), anti-choline acetyltransferase (AB144P, Chemicon), anti-HA (2367, Cell Signaling). Relative signal intensities were quantified by NIH Image J software and are shown in graphs below the corresponding panels.

Histological Analysis

Quadriceps muscles were snap frozen in isopentane. Sections of unfixed muscle tissue were cut at 7 microns in a −28°C cryostat and processed for hematoxylin and eosin or nicotinamide adenine dinucleotide (NADH) staining. Hematoxylin and eosin staining: Slides were incubated in hematoxylin for 3 min, and rinsed in water. They were then stained with eosin, dehydrated through gradient ethanol, then immersed in xylene for 30 minutes followed by mounting in Permount (Electron Microscopy Science, PA). NADH staining: Slides were incubated in NADH and NBT solution in the oven for 1 hour or until the sections become dark. Slides were then rinsed and mounted with Shur/Mount mounting medium (Pella Inc, CA). Motor neuron count: Deeply anesthetized mice were transcardially perfused with 4% paraformaldehyde (PFA). Lumbar spinal cords and proximal hind limbs were dissected, post-fixed for 2 hours in 4% PFA and stored in 70% ethanol. Paraffin-embedded lumbar spinal cord was serially sectioned at 5-μm steps, mounted on slides, and processed for Nissl staining. Images of 10 contiguous sections, 100 μm apart (original magnification, ×10) were analyzed with NIH ImageJ software. Motor neurons were identified as cells positive for Nissl staining, with clear nucleus and nucleolus, with a maximum diameter greater than 20 μm. All neurons in the region below a line drawn horizontally at the level of the spinal canal were measured. Counting was performed in a blinded fashion. Motor neuron cross-sectional area: the distribution of motor neurons was obtained by ranking the neurons by size, and the mean ± s.e.m. of the number of motor neurons of n = 3 animals was calculated for each size range. For statistical analysis, we used Wilcoxon rank sum test with continuity correction to compare distribution differences among genotypes. 1C2 staining: 6-μm-thick tissue sections were deparaffinized and rehydrated through a graded series of alcohol-water solutions, and pretreated with microwave oven heating for 10 minutes in 10 mM citrate buffer at pH 6.0 and then in formic acid for 5 minutes at room temperature. The tissue sections were stained with mouse 1C2 antibody (1:10000) using Envision-plus kit (Dako K2006) according to the manufacturer’s instructions. Sections were counterstained with Mayer's hematoxylin. For the ventral horn of the spinal cord, fifty consecutive transverse sections of the lumbar spinal cord were prepared from each individual mouse and 1C2-positive cells within the ventral horn of every fifth section were counted. For muscle, more than 500 fibers were counted in randomly selected areas of individual mice.

NIH-PA Author Manuscript

NIH-PA Author Manuscript

NIH-PA Author Manuscript

Statistical Analysis

A one-way ANOVA was used to evaluate the effect of IGF-1 among treatment groups. Two-sample t tests were used for *post-hoc* comparisons. A two-way mixed design ANOVA was conducted to compare the effects of genotype on performance at the hanging wire and rotarod tasks as well as on body weight over time. Genotype was used as a between-subjects factor, and time was used as a within-subjects factor. A Fisher's Least Significant Difference (LSD) *post-hoc* was used to compare the performance and body weight across genotypes at each time point. A log rank test was used to compare Kaplan-Meier survival, disease onset and disease duration curves between AR97Q and AR97Q/mIGF-1 genotypes. In these curves data were censored either when a mouse died for a cause independent of SBMA (one mouse died for prolapsed colon and one during blood collection) or when a mouse was sacrificed at a fixed time point for biochemical and histopathological analyses or at the end of the observation period. Censoring is indicated in Figure 5 by a vertical thick mark at the time of the event.

Supplementary Material

Refer to Web version on PubMed Central for supplementary material.

ACKNOWLEDGEMENTS

We thank G. Harmison for skillful technical assistance, Dr. S. Ranganathan and the other members of Dr. Fischbeck's lab for advice and discussion, Dr. A. Lieberman for providing us with control tissue samples, Dr. J. Crawley for advice about mouse behavioral studies, Drs. L. Wrabetz and S. Previtali for kindly providing us with muscle samples from denervated mice, Dr A. Antignani for instructions for size-exclusion chromatography, and Dr. F. Sambataro for statistical analysis. This work was supported by NINDS intramural funds and by grants from Telethon-Italy (GFP04005, M.P.; A.M.), the Kennedy's Disease Association (M.P.), Muscular Dystrophy Association (Development Grant, M.P.; Research Grant, J.P.T.), and the NIH (NS053825, J.P.T.). The authors declare that no conflict of interest exists.

REFERENCES

Alessi DR, Andjelkovic M, Caudwell B, Cron P, Morrice N, Cohen P, Hemmings BA. Mechanism of activation of protein kinase B by insulin and IGF-1. EMBO J 1996;15:6541–6551. [PubMed: 8978681]

Bagriantsev SN, Kushnirov VV, Liebman SW. Analysis of amyloid aggregates using agarose gel electrophoresis. Methods Enzymol 2006;412:33–48. [PubMed: 17046650]

Banno H, Katsuno M, Suzuki K, Takeuchi Y, Kawashima M, Suga N, Takamori M, Ito M, Nakamura T, Matsuo K, et al. Phase 2 trial of leuprorelin in patients with spinal and bulbar muscular atrophy. Ann Neurol 2009;65:140–150. [PubMed: 19259967]

Bodine SC, Stitt TN, Gonzalez M, Kline WO, Stover GL, Bauerlein R, Zlotchenko E, Scrimgeour A, Lawrence JC, Glass DJ, Yancopoulos GD. Akt/mTOR pathway is a crucial regulator of skeletal muscle hypertrophy and can prevent muscle atrophy in vivo. Nat Cell Biol 2001;3:1014–1019. [PubMed: 11715023]

Bonuccelli G, Sotgia F, Capozza F, Gazzerro E, Minetti C, Lisanti MP. Localized treatment with a novel FDA-approved proteasome inhibitor blocks the degradation of dystrophin and dystrophin-associated proteins in mdx mice. Cell Cycle 2007;6:1242–1248. [PubMed: 17495527]

Borasio GD, Robberecht W, Leigh PN, Emile J, Guiloff RJ, Jerusalem F, Silani V, Vos PE, Wokke JH, Dobbins T. European ALS/IGF-I Study Group. A placebo-controlled trial of insulin-like growth factor-I in amyotrophic lateral sclerosis. Neurology 1998;51:583–586. [PubMed: 9710040]

Caroni P, Grandes P. Nerve sprouting in innervated adult skeletal muscle induced by exposure to elevated levels of insulin-like growth factors. J Cell Biol 1990;110:1307–1317. [PubMed: 2157718]

Cary GA, La Spada AR. Androgen receptor function in motor neuron survival and degeneration. Phys Med Rehabil Clin N Am 2008;19:479–494. [PubMed: 18625411]viii.

Coleman ME, DeMayo F, Yin KC, Lee HM, Geske R, Montgomery C, Schwartz RJ. Myogenic vector expression of insulin-like growth factor I stimulates muscle cell differentiation and myofiber hypertrophy in transgenic mice. J Biol Chem 1995;270:12109–12116. [PubMed: 7744859]

NIH-PA Author Manuscript NIH-PA Author Manuscript NIH-PA Author Manuscript

Crawley JN. Behavioral phenotyping strategies for mutant mice. Neuron 2008;57:809–818. [PubMed: 18367082]

DiStefano PS, Friedman B, Radziejewski C, Alexander C, Boland P, Schick CM, Lindsay RM, Wiegand SJ. The neurotrophins BDNF, NT-3, and NGF display distinct patterns of retrograde axonal transport in peripheral and central neurons. Neuron 1992;8:983–993. [PubMed: 1375039]

Dobrowolny G, Giacinti C, Pelosi L, Nicoletti C, Winn N, Barberi L, Molinaro M, Rosenthal N, Musaro A. Muscle expression of a local Igf-1 isoform protects motor neurons in an ALS mouse model. J Cell Biol 2005;168:193–199. [PubMed: 15657392]

Florini JR, Ewton DZ, Coolican SA. Growth hormone and the insulin-like growth factor system in myogenesis. Endocr Rev 1996;17:481–517. [PubMed: 8897022]

Hughes RA, Sendtner M, Thoenen H. Members of several gene families influence survival of rat motoneurons in vitro and in vivo. J Neurosci Res 1993;36:663–671. [PubMed: 8145295]

Humbert S, Bryson EA, Cordelieres FP, Connors NC, Datta SR, Finkbeiner S, Greenberg ME, Saudou F. The IGF-1/Akt pathway is neuroprotective in Huntington's disease and involves Huntingtin phosphorylation by Akt. Dev Cell 2002;2:831–837. [PubMed: 12062094]

Jordan CL, Lieberman AP. Spinal and bulbar muscular atrophy: a motoneuron or muscle disease? Curr Opin Pharmacol 2008;8:752–758. [PubMed: 18775514]

Kaspar BK, Llado J, Sherkat N, Rothstein JD, Gage FH. Retrograde viral delivery of IGF-1 prolongs survival in a mouse ALS model. Science 2003;301:839–842. [PubMed: 12907804]

Katsuno M, Adachi H, Doyu M, Minamiyama M, Sang C, Kobayashi Y, Inukai A, Sobue G. Leuprorelin rescues polyglutamine-dependent phenotypes in a transgenic mouse model of spinal and bulbar muscular atrophy. Nat Med 2003;9:768–773. [PubMed: 12754502]

Katsuno M, Adachi H, Kume A, Li M, Nakagomi Y, Niwa H, Sang C, Kobayashi Y, Doyu M, Sobue G. Testosterone reduction prevents phenotypic expression in a transgenic mouse model of spinal and bulbar muscular atrophy. Neuron 2002;35:843–854. [PubMed: 12372280]

Katsuno M, Adachi H, Waza M, Banno H, Suzuki K, Tanaka F, Doyu M, Sobue G. Pathogenesis, animal models and therapeutics in spinal and bulbar muscular atrophy (SBMA). Exp Neurol 2006;200:8–18. [PubMed: 16513111]

Kostrominova TY, Dow DE, Dennis RG, Miller RA, Faulkner JA. Comparison of gene expression of 2-mo denervated, 2-mo stimulated-denervated, and control rat skeletal muscles. Physiol Genomics 2005;22:227–243. [PubMed: 15840640]

La Spada AR, Wilson EM, Lubahn DB, Harding AE, Fischbeck KH. Androgen receptor gene mutations in X-linked spinal and bulbar muscular atrophy. Nature 1991;352:77–79. [PubMed: 2062380]

Lai EC, Felice KJ, Festoff BW, Gawel MJ, Gelinas DF, Kratz R, Murphy MF, Natter HM, Norris FH, Rudnicki SA. The North America ALS/IGF-I Study Group. Effect of recombinant human insulin-like growth factor-I on progression of ALSA placebo-controlled study. Neurology 1997;49:1621–1630. [PubMed: 9409357]

Lawlor MA, Alessi DR. PKB/Akt: a key mediator of cell proliferation, survival and insulin responses? J Cell Sci 2001;114:2903–2910. [PubMed: 11686294]

Li M, Chevalier-Larsen ES, Merry DE, Diamond MI. Soluble androgen receptor oligomers underlie pathology in a mouse model of spinobulbar muscular atrophy. J Biol Chem 2007;282:3157–3164. [PubMed: 17121819]

Lin HK, Wang L, Hu YC, Altuwaijri S, Chang C. Phosphorylation-dependent ubiquitylation and degradation of androgen receptor by Akt require Mdm2 E3 ligase. EMBO J 2002;21:4037–4048. [PubMed: 12145204]

Lin HK, Yeh S, Kang HY, Chang C. Akt suppresses androgen-induced apoptosis by phosphorylating and inhibiting androgen receptor. Proc Natl Acad Sci U S A 2001;98:7200–7205. [PubMed: 11404460]

Monks DA, Johansen JA, Mo K, Rao P, Eagleson B, Yu Z, Lieberman AP, Breedlove SM, Jordan CL. Overexpression of wild-type androgen receptor in muscle recapitulates polyglutamine disease. Proc Natl Acad Sci U S A 2007;104:18259–18264. [PubMed: 17984063]

Musaro A, McCullagh K, Paul A, Houghton L, Dobrowolny G, Molinaro M, Barton ER, Sweeney HL, Rosenthal N. Localized Igf-1 transgene expression sustains hypertrophy and regeneration in senescent skeletal muscle. Nat Genet 2001;27:195–200. [PubMed: 11175789]

NIH-PA Author Manuscript NIH-PA Author Manuscript NIH-PA Author Manuscript

Neff NT, Prevette D, Houenou LJ, Lewis ME, Glicksman MA, Yin QW, Oppenheim RW. Insulin-like growth factors: putative muscle-derived trophic agents that promote motoneuron survival. J Neurobiol 1993;24:1578–1588. [PubMed: 8301266]

Orr HT, Zoghbi HY. Trinucleotide repeat disorders. Annu Rev Neurosci 2007;30:575–621. [PubMed: 17417937]

Palazzolo I, Burnett BG, Young JE, Brenne PL, La Spada AR, Fischbeck KH, Howell BW, Pennuto M. Akt blocks ligand binding and protects against expanded polyglutamine androgen receptor toxicity. Hum Mol Genet 2007;16:1593–1603. [PubMed: 17470458]

Pennuto M, Tinelli E, Malaguti M, Del Carro U, D'Antonio M, Ron D, Quattrini A, Feltri ML, Wrabetz L. Ablation of the UPR-mediator CHOP restores motor function and reduces demyelination in Charcot-Marie-Tooth 1B mice. Neuron 2008;57:393–405. [PubMed: 18255032]

Rommel C, Bodine SC, Clarke BA, Rossman R, Nunez L, Stitt TN, Yancopoulos GD, Glass DJ. Mediation of IGF-1-induced skeletal myotube hypertrophy by PI(3)K/Akt/mTOR and PI(3)K/Akt/GSK3 pathways. Nat Cell Biol 2001;3:1009–1013. [PubMed: 11715022]

Ross CA, Poirier MA. Protein aggregation and neurodegenerative disease. Nat Med 2004;10:S10–S17. [PubMed: 15272267]

Rusmini P, Sau D, Crippa V, Palazzolo I, Simonini F, Onesto E, Martini L, Poletti A. Aggregation and proteasome: the case of elongated polyglutamine aggregation in spinal and bulbar muscular atrophy. Neurobiol Aging 2007;28:1099–1111. [PubMed: 16781019]

Sandri M. Signaling in muscle atrophy and hypertrophy. Physiology (Bethesda) 2008;23:160–170. [PubMed: 18556469]

Sandri M, Sandri C, Gilbert A, Skurk C, Calabria E, Picard A, Walsh K, Schiaffino S, Lecker SH, Goldberg AL. Foxo transcription factors induce the atrophy-related ubiquitin ligase atrogin-1 and cause skeletal muscle atrophy. Cell 2004;117:399–412. [PubMed: 15109499]

Sarbassov DD, Ali SM, Sabatini DM. Growing roles for the mTOR pathway. Curr Opin Cell Biol 2005;17:596–603. [PubMed: 16226444]

Schmidt BJ, Greenberg CR, Allingham-Hawkins DJ, Spriggs EL. Expression of X-linked bulbospinal muscular atrophy (Kennedy disease) in two homozygous women. Neurology 2002;59:770–772. [PubMed: 12221177]

Soraru G, D'Ascenzo C, Polo A, Palmieri A, Baggio L, Vergani L, Gellera C, Moretto G, Pegoraro E, Angelini C. Spinal and bulbar muscular atrophy: skeletal muscle pathology in male patients and heterozygous females. J Neurol Sci 2008;264:100–105. [PubMed: 17854832]

Sorenson EJ, Windbank AJ, Mandrekar JN, Bamlet WR, Appel SH, Armon C, Barkhaus PE, Bosch P, Boylan K, David WS, et al. Subcutaneous IGF-1 is not beneficial in 2-year ALS trial. Neurology 2008;71:1770–1775. [PubMed: 19029516]

Stenoien DL, Cummings CJ, Adams HP, Mancini MG, Patel K, DeMartino GN, Marcelli M, Weigel NL, Mancini MA. Polyglutamine-expanded androgen receptors form aggregates that sequester heat shock proteins, proteasome components and SRC-1, and are suppressed by the HDJ-2 chaperone. Hum Mol Genet 1999;8:731–741. [PubMed: 10196362]

Stitt TN, Drujan D, Clarke BA, Panaro F, Timofeyva Y, Kline WO, Gonzalez M, Yancopoulos GD, Glass DJ. The IGF-1/PI3K/Akt pathway prevents expression of muscle atrophy-induced ubiquitin ligases by inhibiting FOXO transcription factors. Mol Cell 2004;14:395–403. [PubMed: 15125842]

Taylor JP, Tanaka F, Robitschek J, Sandoval CM, Taye A, Markovic-Plese S, Fischbeck KH. Aggresomes protect cells by enhancing the degradation of toxic polyglutamine-containing protein. Hum Mol Genet 2003;12:749–757. [PubMed: 12651870]

Vlahos CJ, Matter WF, Hui KY, Brown RF. A specific inhibitor of phosphatidylinositol 3-kinase, 2-(4-morpholinyl)-8-phenyl-4H-1-benzopyran-4-one (LY294002). J Biol Chem 1994;269:5241–5248. [PubMed: 8106507]

Williams AJ, Knutson TM, Colomer Gould VF, Paulson HL. In vivo suppression of polyglutamine neurotoxicity by C-terminus of Hsp70-interacting protein (CHIP) supports an aggregation model of pathogenesis. Neurobiol Dis 2009;33:342–353. [PubMed: 19084066]

Yu Z, Dadgar N, Albertelli M, Gruis K, Jordan C, Robins DM, Lieberman AP. Androgen-dependent pathology demonstrates myopathic contribution to the Kennedy disease phenotype in a mouse knock-in model. J Clin Invest 2006;116:2663–2672. [PubMed: 16981011]

NIH-PA Author Manuscript

NIH-PA Author Manuscript

NIH-PA Author Manuscript

Zhao J, Brault JJ, Schild A, Cao P, Sandri M, Schiaffino S, Lecker SH, Goldberg AL. FoxO3 coordinately activates protein degradation by the autophagic/lysosomal and proteasomal pathways in atrophying muscle cells. Cell Metab 2007;6:472–483. [PubMed: 18054316]

Zhu X, Yeadon JE, Burden SJ. AML1 is expressed in skeletal muscle and is regulated by innervation. Mol Cell Biol 1994;14:8051–8057. [PubMed: 7969143]

NIH-PA Author Manuscript

NIH-PA Author Manuscript

NIH-PA Author Manuscript

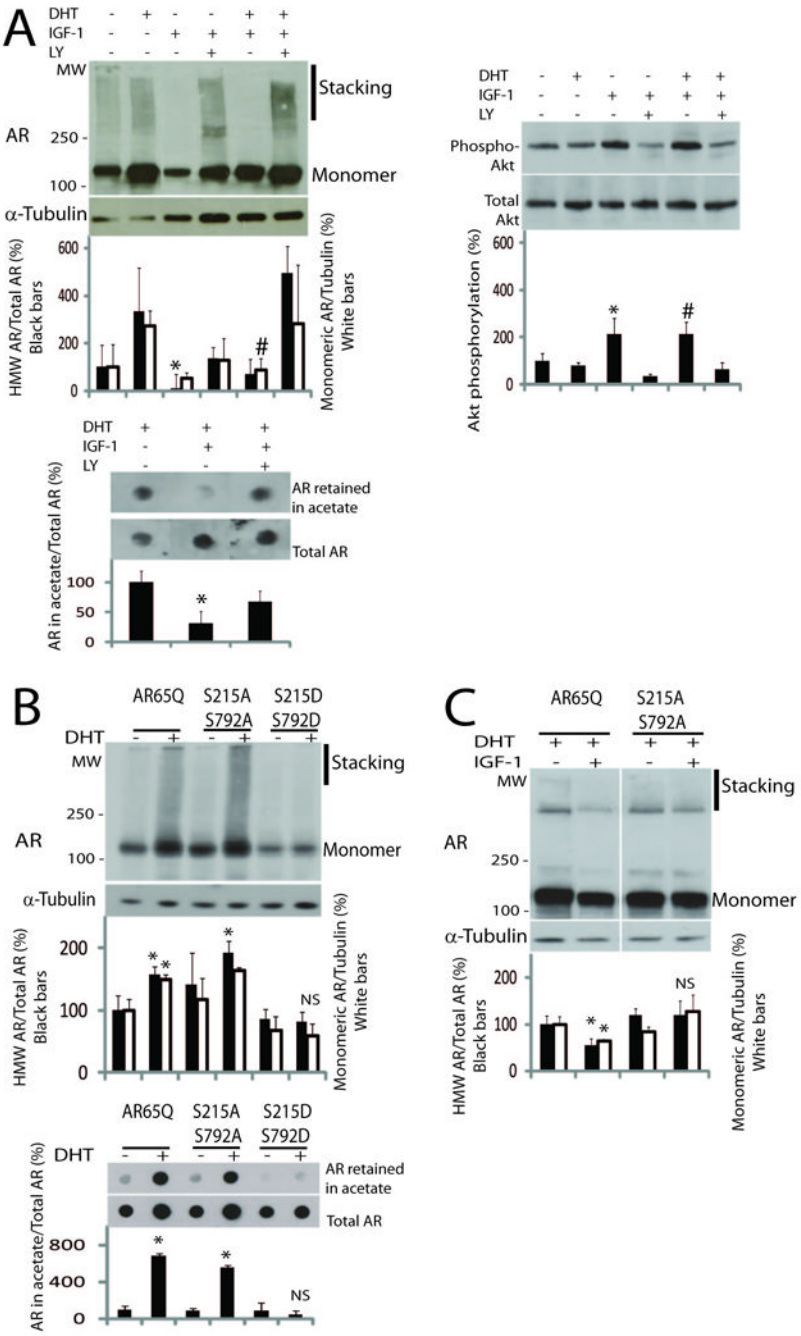

Figure 1. IGF-1 Decreases AR Aggregation in Cultured Cells through Activation of the PI3K/Akt Pathway and Phosphorylation of AR by Akt

(A) Analysis of AR aggregation in COS1 cells transfected with vector expressing mutant AR with 65 glutamine residues (AR65Q) and treated with DHT, LY294002 (LY), and IGF-1 by western blotting (top panel) and filter retardation assay (bottom panel). DHT increased the accumulation of both high molecular weight (HMW) AR species (black bars) and monomeric AR (white bars). IGF-1 decreased both the basal and ligand-induced accumulation of HMW and monomeric AR, and this effect was reduced by the PI3K inhibitor LY294002. Graphs, mean ± s.e.m., n = 4, (top panel) * p = 0.01 relative to non-stimulated AR65Q–expressing cells (black bars), and # p = 0.004 relative to DHT-treated cells (white bars), (bottom panel) * p =

NIH-PA Author Manuscript

NIH-PA Author Manuscript

NIH-PA Author Manuscript

0.003, (post-hoc t test). AR was detected with antibody to AR (N20). α-Tubulin is shown as loading control. MW, molecular weight. (Right panel) Phosphorylation of Akt was analyzed by western blotting under the same experimental conditions with anti-phospho-serine 473 and anti-total Akt antibodies. Phosphorylation of Akt is represented as the ratio of the signals detected with anti-phospho-serine and total Akt antibodies. Graph, mean ± s.e.m., n = 4, * p = 0.05, # p = 0.01.

(B) Western analysis (upper panel) and filter retardation assay (bottom panel) showed that DHT increased the accumulation of both HMW AR species (black bars) and monomeric AR (white bars) in COS1 cells expressing AR65Q and AR65Q with alanine substitutions for serine 215 and serine 792 (S215A,S792A), but not in cells expressing AR with aspartate substitutions (S215D,S792D). Graphs, mean ± s.e.m., n = 3, (top panel) * p = 0.01, (bottom panel) * p = 0.05, NS non-significant relative to the non-stimulated sample expressing AR65Q (post-hoc t test).

(C) Western analysis of HEK293T cells treated with DHT and IGF-1 revealed that IGF-1 decreases the accumulation of HMW (black bars) and monomeric (white bars) AR in cells expressing AR65Q, but not the alanine-substituted receptor. Graph, mean ± s.e.m., n = 3, * p = 0.01 and NS non-significant (post-hoc t test) relative to the corresponding DHT-treated sample. In (A, B, and C) the first sample is represented as 100%.

NIH-PA Author Manuscript

NIH-PA Author Manuscript

NIH-PA Author Manuscript

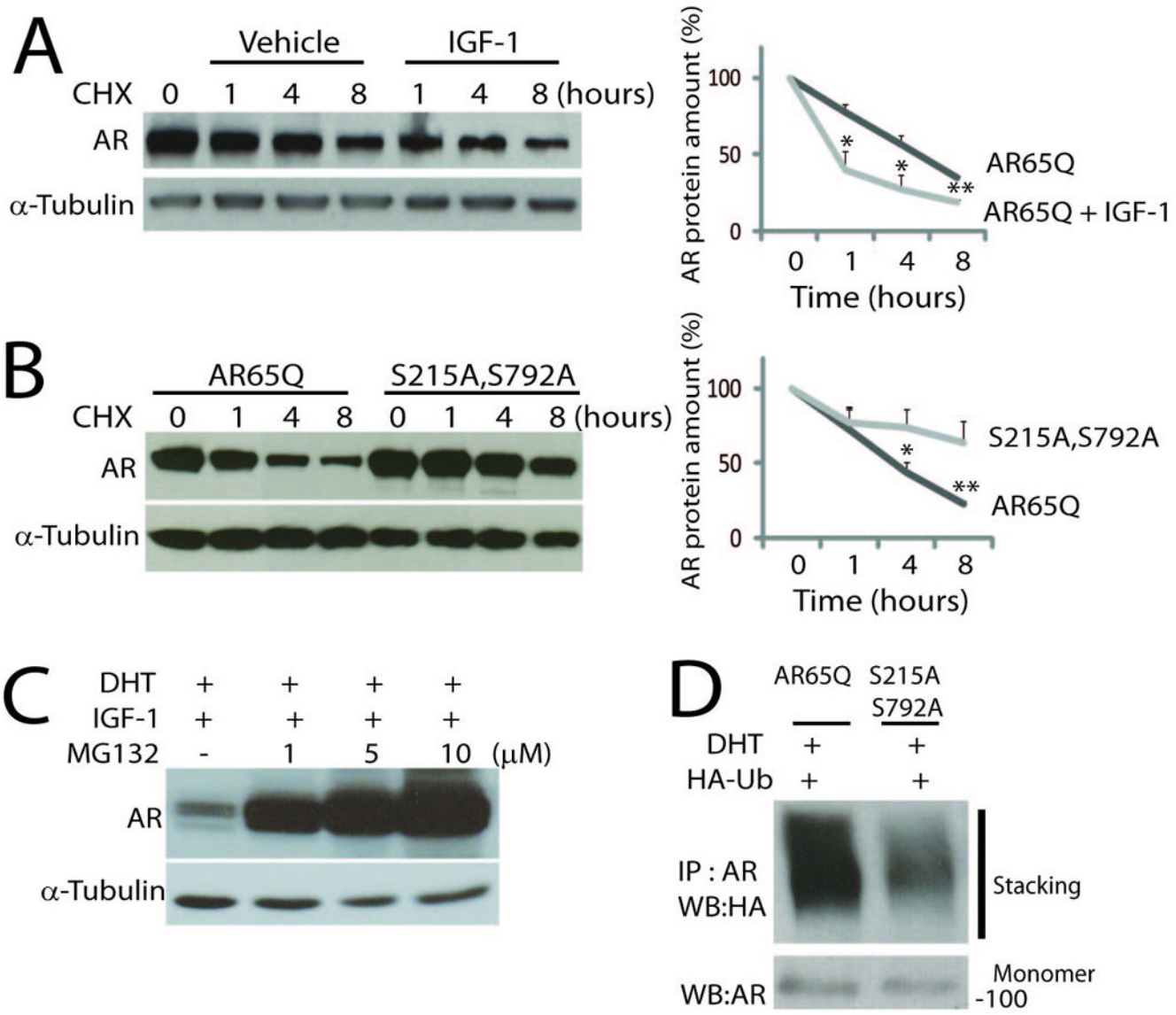

Figure 2. IGF-1 Promotes Mutant AR Clearance Through the Ubiquitin-Proteasome System

(A) Western analysis of MN-1 cells transfected with AR65Q and incubated with cycloheximide (CHX) for 1, 4, and 8 hours in the presence and absence of IGF-1 showed that IGF-1 increases the rate of AR clearance. Graph, mean ± s.e.m., n = 3, * p = 0.03, ** p = 0.001 (student's t test).

(B) Western analysis of HEK293T cells transfected as indicated and treated with CHX showed that the clearance of the alanine-substituted receptor is slower than AR65Q. Graph, mean ± s.e.m., n = 5, * p = 0.04, **p = 0.01.

(C) Western analysis of MN-1 cells expressing AR65Q and treated with DHT, IGF-1, and the proteasome inhibitor MG132 showed that the IGF-1-induced clearance of AR65Q is blocked by MG132 in a dose-dependent fashion. Shown is one experiment representative of 3.

(D) Immunoprecipitation with anti-AR antibody of HEK293T cells expressing the indicated AR65Q versions together with HA-tagged ubiquitin (HA-Ub), followed by western analysis with anti-HA or AR antibodies, showed reduced ubiquitylation of the alanine-substituted receptor. Shown is one experiment representative of 4.

NIH-PA Author Manuscript

NIH-PA Author Manuscript

NIH-PA Author Manuscript

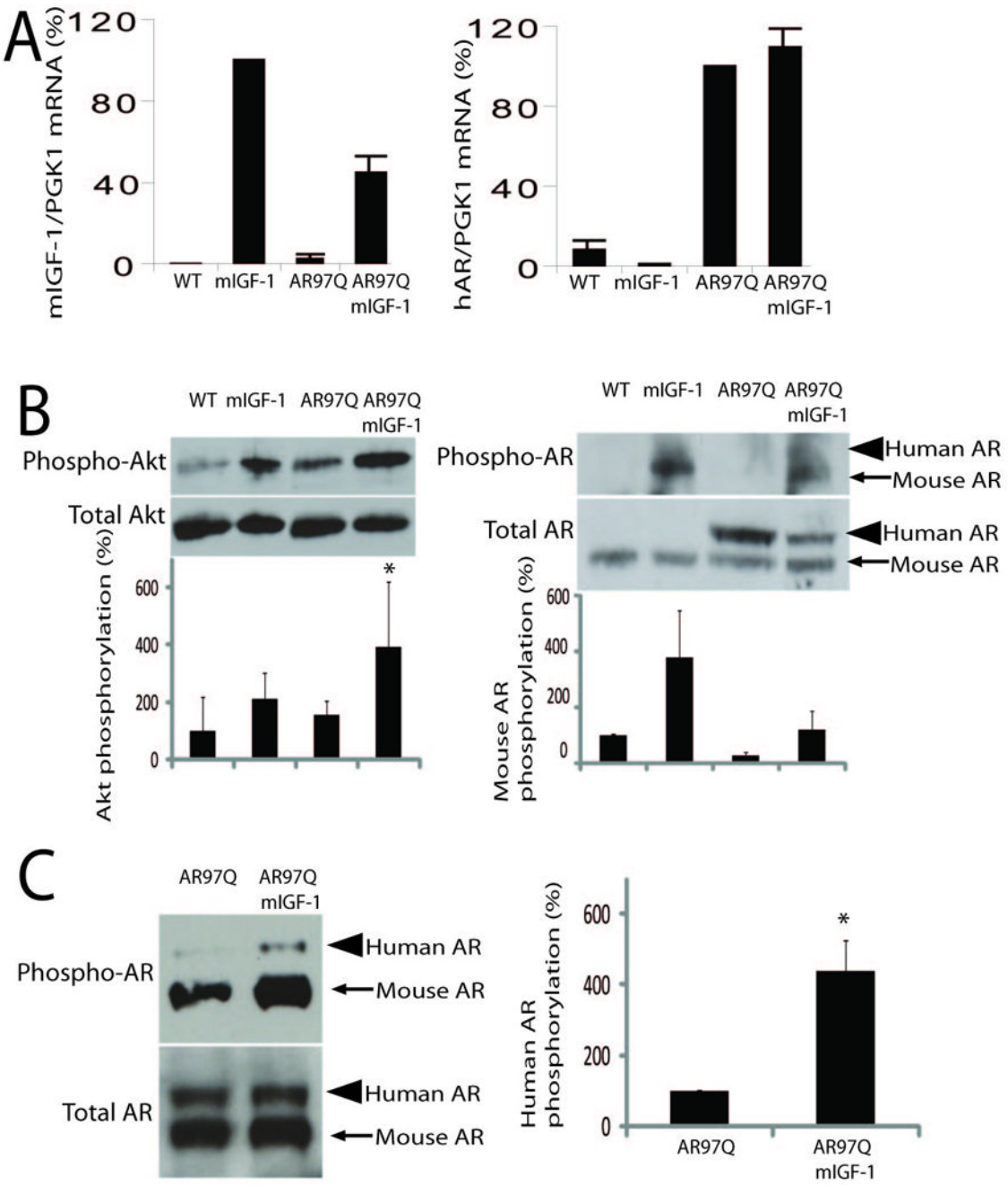

Figure 3. mIGF-1 Stimulates Phosphorylation of Akt and AR in SBMA Muscle

(A) Rat mIGF-1 (left panel) and human AR (right panel) mRNA levels were measured by quantitative real-time PCR in skeletal muscle of 12 weeks old mice. mIGF-1 is expressed in both AR97Q/mIGF-1 and mIGF-1 mice. AR97Q is expressed in both AR97Q and AR97Q/mIGF-1 mice. Data were normalized to phosphoglycerate kinase (PGK1) mRNA. Data are represented relative to mIGF-1 mice = 100% (left) and to AR97Q mice = 100% (right). Graphs, mean ± s.e.m.; n = 3.

(B) Western analysis to detect phosphorylation at serine 473 of Akt (left panel) and serine 215 of AR (right panel) was performed using specific phospho-serine antibodies in the skeletal

NIH-PA Author Manuscript

NIH-PA Author Manuscript

NIH-PA Author Manuscript

muscle of 6 (left) and 12 (right) weeks old mice. Total Akt and AR were measured as loading control. Graphs, mean ± s.e.m., n = 5 right panel, n = 3 left panel, * p = 0.04.

(C) Western analysis of skeletal muscle from AR97Q and AR97Q/mIGF-1 mice injected with the proteasome inhibitor velcade showed increased phosphorylation of human expanded polyglutamine AR in mice overexpressing mIGF-1. Graphs, mean ± s.e.m., n = 3, * p = 0.01. In (B and C) the first sample is represented as 100%.

NIH-PA Author Manuscript

NIH-PA Author Manuscript

NIH-PA Author Manuscript

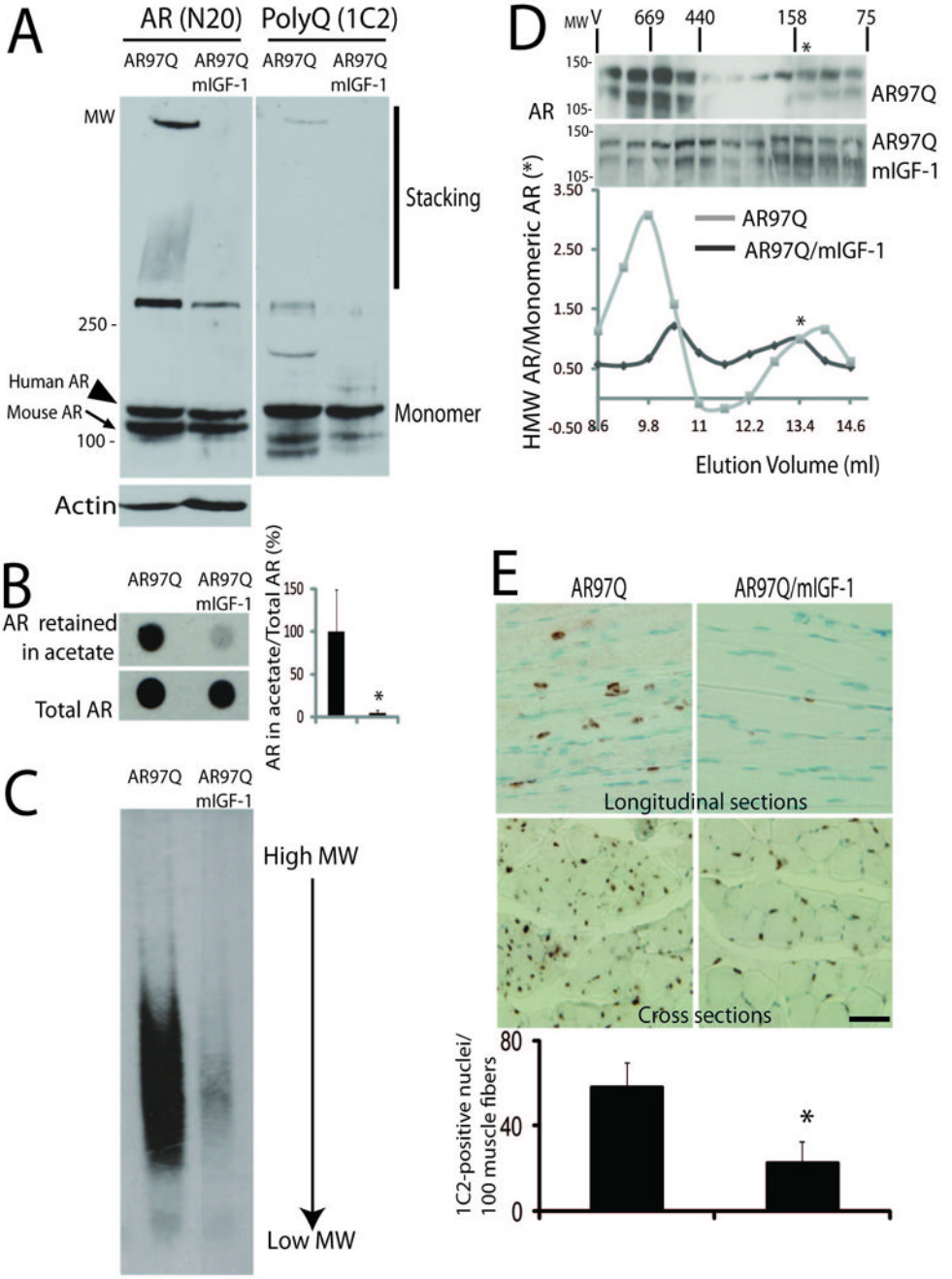

Figure 4. mIGF-1 Reduces AR Aggregation in SBMA Muscle

(A) Western blotting and (B) filter retardation assay analyses showed a reduction in the accumulation of high molecular weight AR species in the skeletal muscle of AR97Q/mIGF-1 mice at 12 weeks of age as compared to AR97Q mice. Endogenous and expanded polyglutamine AR were detected with N20 antibody, and expanded polyglutamine AR with 1C2 antibody. Actin was used as a loading control. Shown is one experiment representative of 4 in (A) and of 3 in (B). Graphs, mean ± s.e.m., n = 3, * p = 0.001.

(C) 1.5% SDS-agarose gel analysis revealed that the amount of AR aggregates in the muscle of AR97Q mice was reduced in AR97Q/mIGF-1 mice.

NIH-PA Author Manuscript

NIH-PA Author Manuscript

NIH-PA Author Manuscript

(D) Size-exclusion chromatography (SEC) and western blotting analysis of muscle lysates showed that IGF-1 reduces the amount of AR eluting off as high molecular weight species (fractions 1–4) in AR97Q/mIGF-1 mice compared to AR97Q mice. The horizontal MW markers (kDa) were obtained by SEC analysis of protein standards. V, void volume. The graph shows the ratio between the high molecular weight AR species and monomeric AR, which eluted off as fraction 9 (asterisk). Shown is one experiment, which was representative of 3.
(E) Immunohistochemical analysis using 1C2 antibody on longitudinal and cross sections of AR97Q and AR97Q/mIGF-1 muscle showed a reduction of diffuse nuclear staining and nuclear inclusions in AR97Q/mIGF-1 compared to AR97Q mice. Graphs, mean ± s.e.m.; n = 5, * p = 0.04.Bar, 2 μm.

NIH-PA Author Manuscript

NIH-PA Author Manuscript

NIH-PA Author Manuscript

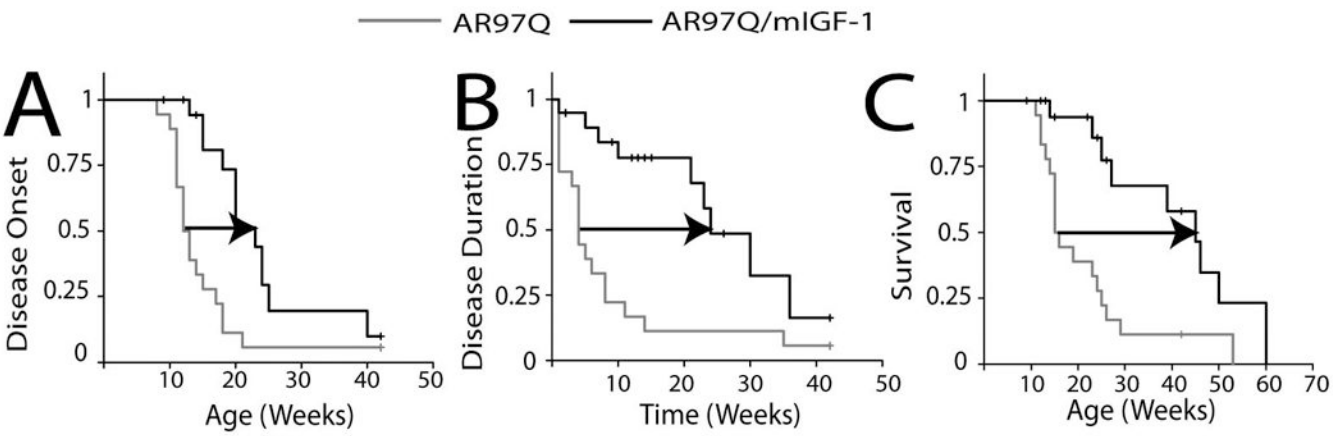

Figure 5. mIGF-1 Delays Disease Onset and Extends Disease Duration and Survival of SBMA Mice

Kaplan-Meier analysis of disease onset (A), disease duration (B) and survival (C) in AR97Q and AR97Q/mIGF-1 mice. (A) The median disease onset - the week in which the mouse starts to lose 5% body weight - was delayed by 10.5 weeks (arrow) in AR97Q/mIGF-1 mice relative to AR97Q mice. (B) The median disease duration - the time interval from disease onset to death - was extended by 20 weeks (arrow) in AR97Q/mIGF-1 mice compared to AR97Q mice. (C) Survival analysis showed that the median lifespan of AR97Q mice was extended by 30 weeks (arrow) in AR97Q/mIGF-1 mice. AR97Q n = 18, AR97Q/mIGF-1 n = 19. Censored data are indicated by the symbol “I” (See Experimental Procedures).

NIH-PA Author Manuscript

NIH-PA Author Manuscript

NIH-PA Author Manuscript

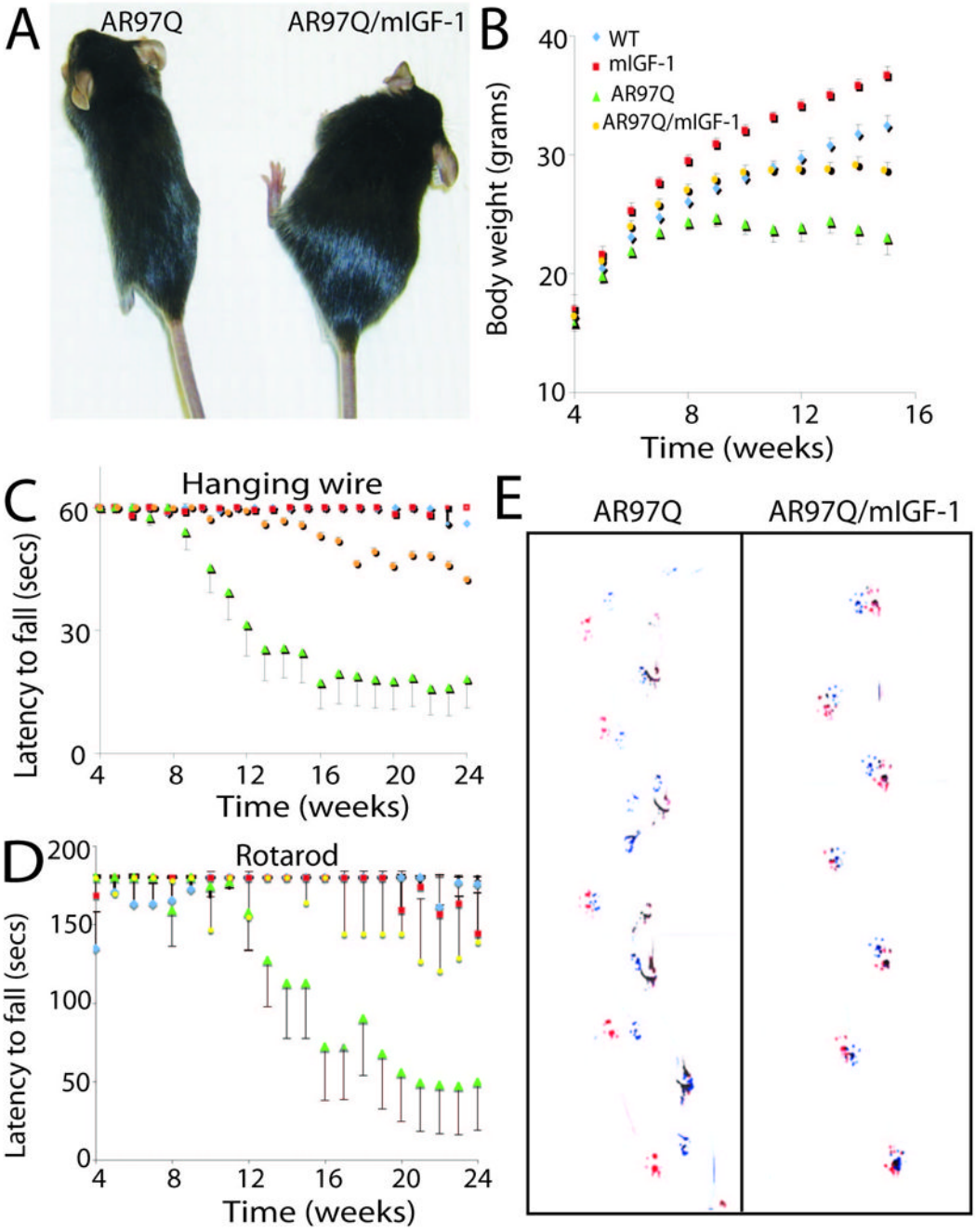

Figure 6. Overexpression of mIGF-1 Attenuates Behavioral Abnormalities in SBMA Mice

(A and B) Body weight analysis showed that AR97Q mice progressively lose body weight starting from 8 weeks of age. AR97Q/mIGF-1 mice have normal body weight up to 12 weeks of age, and do not show body weight loss until 16 weeks of age. Bars, s.e.m., n = 15.

(C) Hanging wire (n = 15) and (D) rotarod (n = 7) analysis showed progressive deterioration in performance of AR97Q mice, which was delayed and improved in AR97Q/mIGF-1 mice. Bars, s.e.m.

(E) Footprints of 12 weeks old mice showed that AR97Q mice dragged hind legs, whereas AR97Q/mIGF-1 mice did not show defects in coordination of steps. Red, front paws; blue, hind paws. Shown is one experiment representative of three.

NIH-PA Author Manuscript

NIH-PA Author Manuscript

NIH-PA Author Manuscript

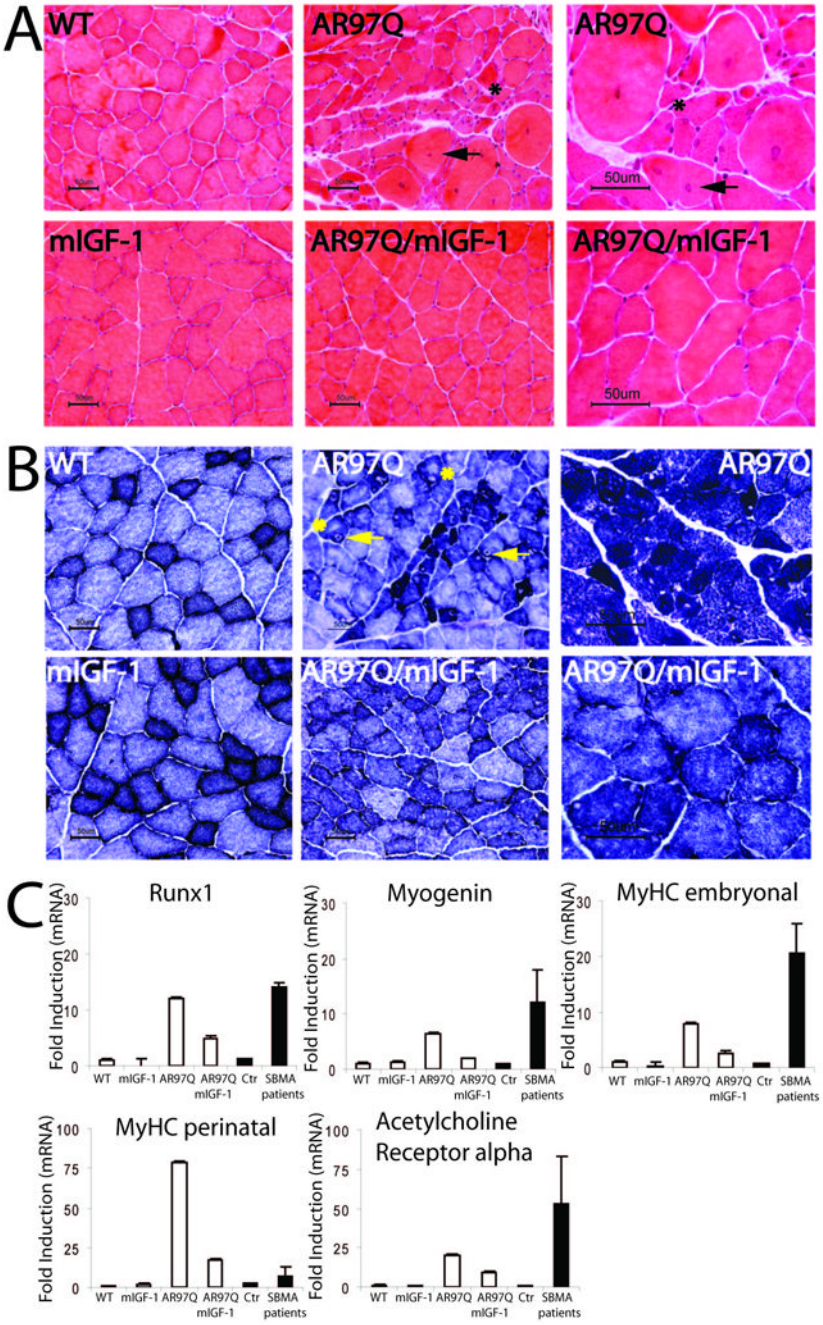

Figure 7. mIGF-1 Ameliorates SBMA Muscle Pathology

(A) Hematoxylin and eosin and (B) nicotinamide adenine dinucleotide staining of transverse sections of quadriceps of 12 weeks old mice. (A) Arrows = fibers with central nuclei; asterisks = angulated and grouped fibers. (B) Arrows = target fibers; asterisks = moth eaten fibers. Shown is one experiment representative of 3.

(C) The mRNA levels of runx1, myogenin, myosin heavy chain (MyHC) embryonal and perinatal, and acetylcholine receptor alpha were measured by real-time PCR in the skeletal muscle of 12 weeks old mice and SBMA patients. Data from mice and patients were normalized to PGK1 and beta-glucoronidase mRNA, respectively. Data are represented relative to wild type mice or control human samples = 1. Graphs, mean ± s.e.m., n = 3 mice and n = 4 patients).

NIH-PA Author Manuscript

NIH-PA Author Manuscript

NIH-PA Author Manuscript

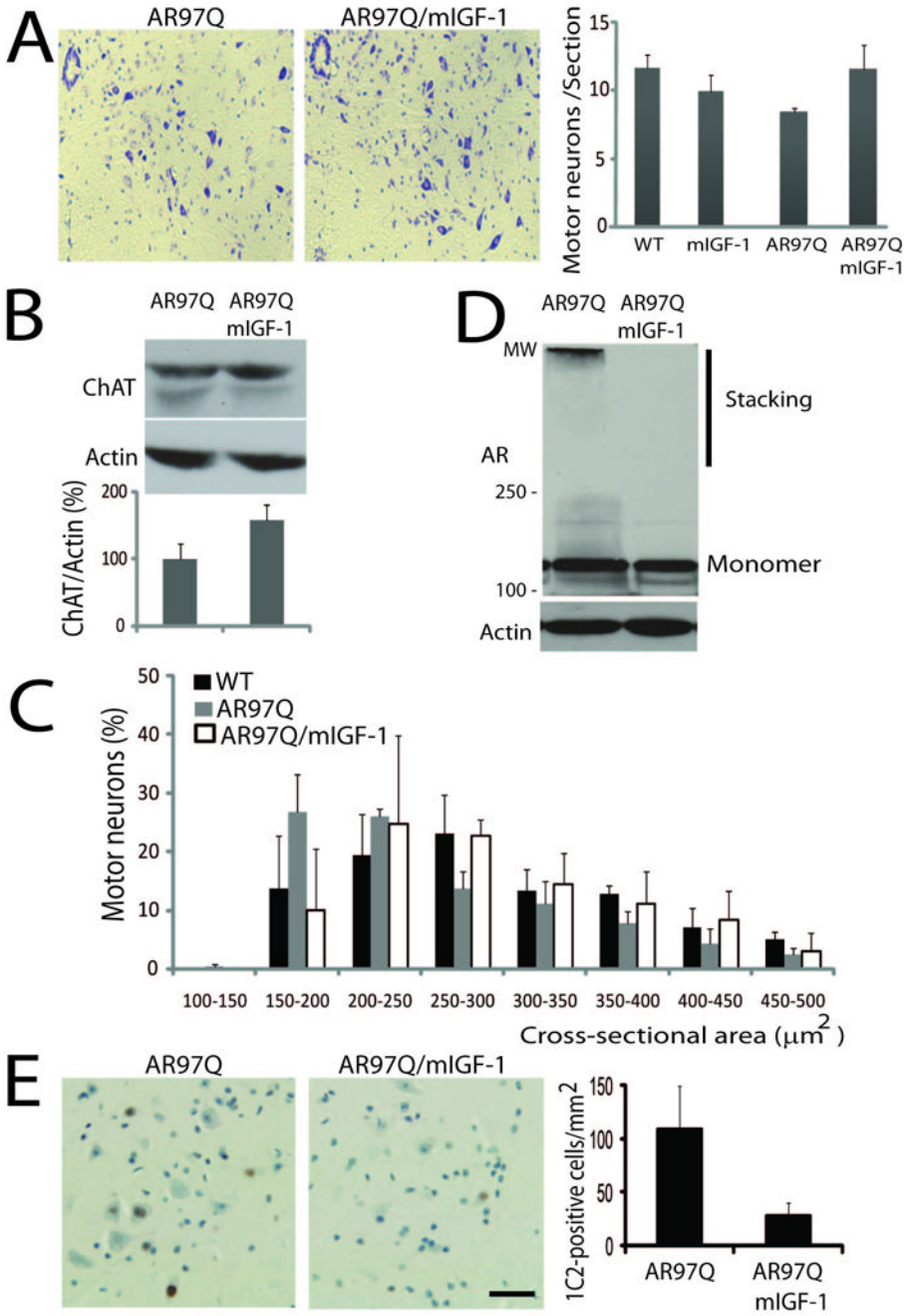

Figure 8. mIGF-1 Reduces Spinal Cord Pathology in SBMA Mice

(A) Nissl-stained transverse sections of ventral spinal cords of 12 weeks old mice. Quantitative analysis showed that the number of motor neurons/section is increased in AR97Q/mIGF-1 mice as compared to AR97Q mice. Graphs, mean ± s.e.m., n = 3.

(B) Western analysis showed that expression of choline acetyltransferase (ChAT) is increased in the spinal cord of 12 weeks old AR97Q/mIGF-1 mice as compared to AR97Q mice. Graphs, mean ± s.e.m., n = 3. The first sample is represented as 100%.

(C) Histograms of the cross-sectional area of motor neurons (See Experimental Procedures). The distribution of motor neuron area is altered in AR97Q mice, but not in AR97Q/mIGF-1 mice relative to wild type mice. Graphs, mean ± s.e.m., n = 3 animals.

NIH-PA Author Manuscript

NIH-PA Author Manuscript

NIH-PA Author Manuscript

(D) Western analysis revealed that AR aggregation is decreased in the spinal cord of AR97Q/mIGF-1 mice as compared to AR97Q mice at 12 weeks of age. AR was detected with N20 antibody. Actin is shown as loading control. Shown is one experiment representative of 3.
(E) Immunohistochemical analysis using 1C2 antibody on cross sections of AR97Q and AR97Q/mIGF-1 ventral spinal cord showed a reduction of nuclear inclusions in AR97Q/mIGF-1 relative to AR97Q mice. Graphs, mean ± s.e.m., n = 4. Bar, 2 μm.